Reductive dearomatization of a substituted benzene triggered by a strong oxidant†

Runyu Tan and Datong Song*

Received 16th September 2009, Accepted 18th September 2009
First published as an Advance Article on the web 6th October 2009
DOI: 10.1039/b919233f

Two new dinuclear platinum complexes $Pt_2Ph_4L^{Et}$ (**1a**) and $Pt_2Ph_4L^{F}$ (**1b**) (where L^{Et} is 1,2,4,5-tetrakis(6-ethylquinolin-8-yl)benzene and L^{F} is 1,2,4,5-tetrakis(6-trifluoromethoxylquinolin-8-yl)benzene) were synthesized and characterized. Triggered by an oxidant NCS, **1a** and **1b** displayed interesting reactivity of reductive dearomatization of the central phenyl rings of L^{Et} and L^{F} ligands respectively. The preliminary radical scavenger test gave some mechanistic insights.

Introduction

Reductive dearomatization of a benzene ring represents one of the most challenging chemical processes due to the kinetic inertness of benzene.[1] Such reduction usually requires strong reductants and harsh conditions, such as sodium in liquid ammonia (Birch reduction),[2a] lithium di-*tert*-butylbiphenyl,[2b] and K/KC_8 with 18-crown-6,[2c] in a moisture- and air-free environment. In contrast, a harder-to-reduce small molecule, dinitrogen, can be reduced to ammonia at the active site of nitrogenase under mild conditions using H_2 as the reductant, owing to the multimetallic feature of the metalloenzyme.[3] Inspired by Nature's strategy for small molecule activation using the cooperation between multiple metal centres, Wang and co-workers have developed a diplatinum complex Pt_2Me_4(ttab) (where ttab = 1,2,4,5-tetrakis(7-azaindol-1-yl)benzene), which is able to reductively dearomatize a substituted benzene ring *via* the joint action between two platinum centers.[4] Thus, Pt_2Me_4(ttab) readily undergoes a tandem C–Cl activation and dearomatization reaction at ambient temperature when treated with chloroform. In this process, a dinuclear Pt(III) species resulting from chlorine atom abstraction by the Pt(II) species from chloroform is believed to be the key intermediate responsible for the subsequent dearomatization. However, the possibility of a dinuclear mixed valence Pt(III)–Pt(IV) intermediate could not be ruled out.[5] To generalize such an interesting reactivity, we designed a series of analogous diplatinum compounds of quinolyl-functionalized tetradentate ligands. These compounds indeed show similar tandem C–Cl activation and dearomatization reactivities (Scheme 1).[6] We were hoping that the alkyl and alkoxy substituents on the tetradentate ligands could solve the solubility problem encountered in mechanistic studies of the dearomatization reaction. Unfortunately, the dimethyl platinum(II) complexes of these ligands did not show good solubility in common solvents. Recently, we have prepared the diphenyl counterparts, $Pt_2Ph_4L^{Et}$ (**1a**) and $Pt_2Ph_4L^{F}$ (**1b**), where L^{Et} and L^{F} are the tetradentate ligands depicted in Scheme 1 with $-C_2H_5$ and $-OCF_3$ substituents, respectively, and observed reasonable solubility. We envisioned that **1a** and **1b** should be less reactive with respect to C–Cl activation compared to their $PtMe_2$ analogues. This may allow us to conduct the reactions in a more controlled fashion, shining light on the mechanism. Herein we report both stoichiometric and catalytic reductive dearomatization reactions by complexes **1** triggered by a strong oxidant *N*-succinimide (NCS) and some new mechanistic information.

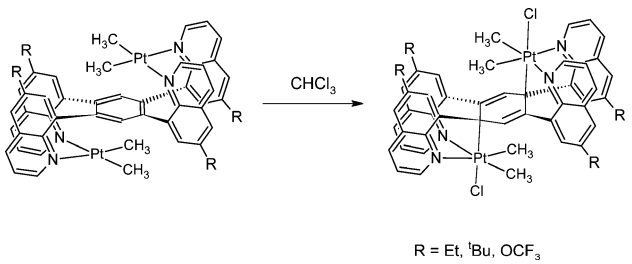

Scheme 1 Tandem C–Cl activation and dearomatization.

Results and discussion

Syntheses and structures of 1a and 1b

Complexes **1a** and **1b** can be synthesized by reacting $[PtPh_2(SMe_2)]_n$ (n = 2 or 3)[7] with L^{Et} and L^{F}, respectively, in nearly quantitative yields (Scheme 2). They are stable at ambient temperature in air in the solid state and solution. The ^{1}H NMR spectra of complexes **1** in CD_2Cl_2 indicate symmetric structures. Thus, there is only one set of quinolinyl signals in the aromatic region at ambient temperature. While the three different proton signals of the phenyl rings directly attached to platinum were well resolved in **1a**, only two multiplets at 6.59–6.75 ppm were observed for **1b**. The solid state structures of **1a** and **1b** have been confirmed by X-ray crystallography. As shown in Fig. 1, both **1a** and **1b** are dinuclear with the central phenyl ring of the chelate ligand sandwiched in between the two Pt(II) centres, displaying a 'S'-shaped spatial arrangement. Each molecule of **1b** has a crystallographically imposed inversion centre, while **1a** does not. Each Pt(II) centre of **1a** and **1b** adopts a typical square-planar geometry, with two nitrogen donor atoms from the two

Davenport Chemical Research Laboratories, Department of Chemistry, University of Toronto, 80 St. George Street, Ontario, Canada M5S 3H6. E-mail: dsong@chem.utoronto.ca; Fax: 1-416-978-7013; Tel: 1-416-978-7014

† CCDC reference numbers 743627 and 743628, 747774 and 747775. For crystallographic data in CIF or other electronic format see DOI: 10.1039/b919233f

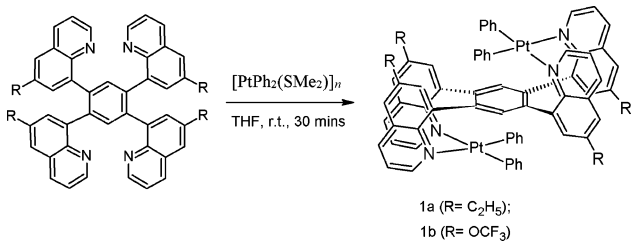

Scheme 2 Syntheses of **1a** and **1b**.

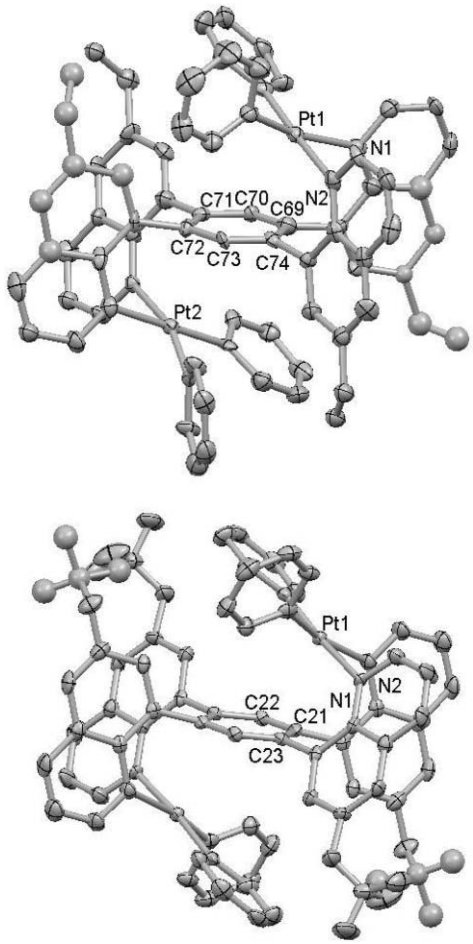

Fig. 1 Molecular structures of **1a** (top) and **1b** (bottom). Thermal ellipsoids are plotted at 50% probability. All hydrogen atoms are omitted for clarity. Only one orientation is shown for the disordered portions.

mutually *ortho* quinolinyl groups of the tetradentate ligand and two carbon donor atoms from two phenyl ligands occupying the four coordination sites in a *cis*-fashion. The Pt–C and Pt–N bond lengths are similar to those in Pt_2Ph_4(ttab).[4] The intramolecular Pt–Pt distances in **1a** and **1b** are 6.5796(6) and 6.6664(7) Å, respectively, significantly shorter than the corresponding distance (7.232(1) Å) in Pt_2(ttab)Ph_4. The dihedral angles between the Pt coordination plane and the central phenyl ring are ~28° and ~30° in **1a** and **1b**, respectively, greater than their corresponding dimethyl platinum counterparts.

Stoichiometric transformations of 1 to 2

In sharp contrast to $Pt_2(CH_3)_4$(ttab), Pt_2Ph_4(ttab), $Pt_2(CH_3)_4L^{Et}$, and $Pt_2(CH_3)_4L^F$, which readily react with chlorinated solvents, **1a** and **1b** show high stability in CH_2Cl_2 and $CHCl_3$. For instance, they remain unchanged after prolonged heating at 70 °C in $CDCl_3$ as monitored by ^{1}H NMR spectroscopy. Since the tandem C–Cl bond cleavage and dearomatization reaction would have to go through a Pt(II) to Pt(III) oxidation, the inertness of compounds **1a** and **1b** towards CH_2Cl_2 and $CHCl_3$ is presumably because of the lower electron density on the Pt centres compared to the dimethyl platinum analogues. We envision that a more oxidizing chlorine atom donor might be able to invoke the Pt(III) intermediate, which in turn, would reduce and dearomatize the central benzene ring of the tetradentate ligand. Benzoyl chloride and trityl chloride were tested first, however, neither reacts with **1a** or **1b**. *N*-Chlorosuccinimide (NCS) is known as a chlorinating reagent that readily oxidizes Pd(II) to Pd(IV),[8] and Pt(II) to Pt(III) and Pt(IV).[9] The reactions between **1a**/**1b** and NCS were then investigated (Scheme 3). The attempt to monitor the reaction between **1a** and NCS by NMR spectroscopy was unsuccessful presumably because of the poor solubility of the product and the existence of side-reactions such as chlorination of the ethyl groups in **1a** by NCS. Fortunately, an appreciable amount of X-ray quality yellow crystals were formed in the NMR tube upon standing for ~30 min. The crystals have been confirmed to be the expected product **2a** by X-ray crystallography and elemental analysis. No NMR data were obtained because of the poor solubility of **2a**.

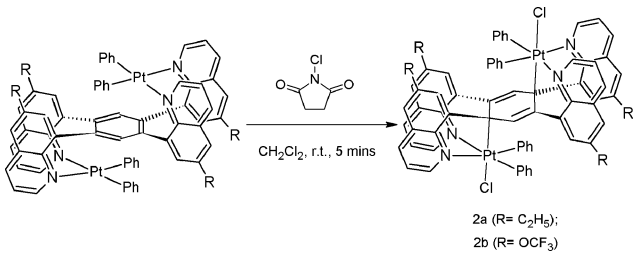

Scheme 3 Reactivity of **1a** and **1b**, formation of **2a** and **2b**.

Unlike **1a**, the treatment of **1b** with NCS (2 equiv. or excess) in CD_2Cl_2 at ambient temperature leads to the quantitative formation of **2b** as observed in the ^{1}H NMR spectrum. For example, the signal at 6.76 ppm with two sets of platinum satellites is characteristic for a cyclohexadiene ring bound to two Pt(IV) centres as previously observed, indicating the successful reductive dearomatization of the central benzene ring of the L^F ligand. The Pt–H coupling constants ($^3J_{Pt-H}$ = 32.4 Hz, $^4J_{Pt-H}$ = 16.4 Hz) are comparable to those observed previously.[6] The quinolinyl groups are no longer equivalent after the formation of the two extra Pt–C bonds, consistent with the two sets of quinolinyl signals in the ^{1}H NMR spectrum. Accordingly, two fluorine shifts can be observed in ^{19}F NMR spectrum of **2b**.

The solid state structures of **2a** and **2b** have been established by X-ray crystallography and are shown in Fig. 2. Each molecule of **2a** and **2b** possesses a crystallographically imposed inversion centre. The central benzene ring retains its planarity and is again situated between two Pt centres, making an extra Pt–C bond to each metal centre compared to those in complexes **1a** and **1b**. Each Pt(IV) centre adopts a distorted-octahedral coordination geometry, with

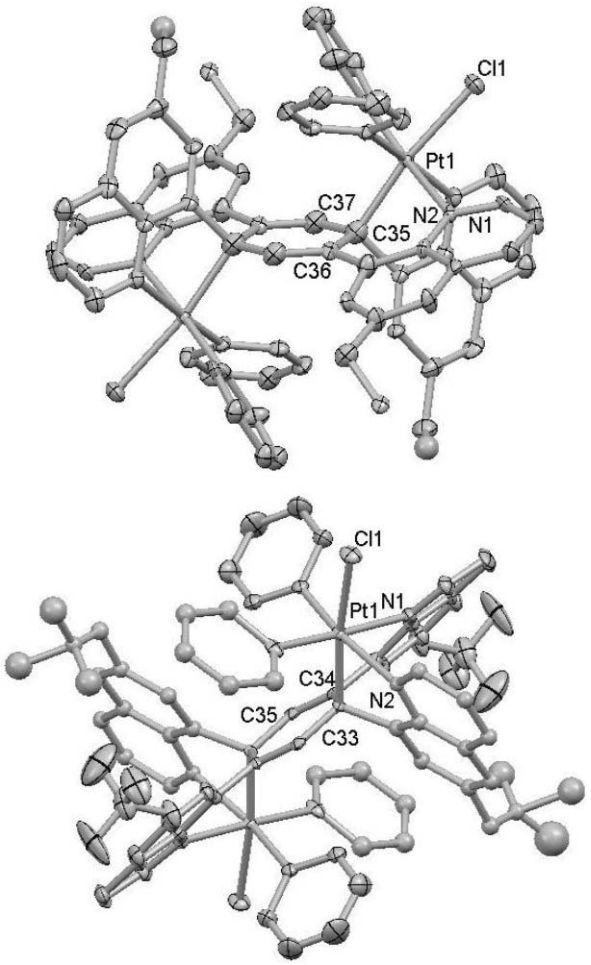

Fig. 2 Molecular structures of **2a** (top) and **2b** (bottom). Thermal ellipsoids are plotted at 50% probability. All hydrogen atoms are omitted for clarity. Only one orientation is shown for the disordered portions.

two nitrogen donor atoms from the chelating ligand, two carbon donor atoms from two phenyl ligands, one chloride, and one carbon donor from the central C_6 ring of the ligand occupying the six coordination sites. The bond lengths and angles around the Pt(IV) centres are similar to those observed previously.[4] Although the central C_6 ring of the chelating ligand is still planar, it is no longer aromatic as indicated by the bond lengths, *i.e.*, two C–C double bonds (1.342(9)–1.352(7) Å) and four C–C single bonds (1.480(7)–1.494(9) Å). The average bond angles around the Pt-bound carbon atoms of the central benzene ring are ~109° for both **2a** and **2b**, showing typical sp^3 character. All these structural features are consistent with the cyclohexadiene dianions observed previously.[4,6]

Transformation of 1b to 2b catalyzed by NCS

The above stoichiometric experiments imply that NCS is a competent chlorine atom donor and helps oxidize Pt(II) to Pt(III). Such a donation of a chlorine atom should produce a succinimide radical, which has been proposed as a potent radical chain carrier.[10] If NCS could be regenerated from a succinimide radical, this transformation would only require a catalytic amount of NCS. Indeed, when **1b** is mixed with chloroform, the introduction of a catalytic amount of NCS leads to the complete conversion of **1b** to **2b** (eqn (1)). Presumably in such a reaction the succinimide radical abstracts a chlorine atom from chloroform and regenerates NCS to turn the catalytic cycle over. Meanwhile, a $CHCl_2$ radical should be produced in such a transformation. Evidently, an appreciable amount of 1,1,2,2-tetrachloroethane was detected in the reaction mixture by GCMS, as a result of the coupling of two $CHCl_2$ radicals. The catalytic transformation from **1b** to **2b** can be completely inhibited by the addition of a radical scavenger 3,5-di-*tert*-butyl-4-hydroxytoluene (BHT),[11] further supporting the radical chain hypothesis.

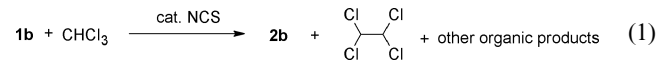

(1)

Probing the reaction mechanism

We chose the stoichiometric reaction of **2b** and NCS to investigate the possible mechanism because the reaction is clean and can be monitored by ^{1}H NMR. The goal of this study is to distinguish between the two mechanistic proposals[5] depicted in Scheme 4, namely the double Pt(III) pathway (route 1) and the Pt(III)–Pt(IV) pathway (route 2). The addition of an excess amount of BHT to the solution of **1b** prior to the addition of NCS does not inhibit the reductive dearomatization. Such experimental results are consistent with route 1, which involves a dinuclear Pt(III) intermediate *ii*. This intermediate does not have well-exposed Pt(III) metalloradicals, because the vacant sites on the metal centres are completely blocked by the central phenyl ring of the chelating ligand. The addition of BHT would not affect the quantitative formation of **2b**. If the reaction proceeds *via* route 2, which involves a dinuclear Pt(III)–Pt(IV) intermediate *iii* with a well-exposed Pt(III) metalloradical, the addition of BHT could quench such a radical, preventing the formation of **2b**. This is inconsistent with our experimental observations.

Conclusion

In summary, two new dinuclear diphenylplatinum(II) complexes **1a** and **1b** of the L ligands display interesting reactivities of reductive dearomatization of a substituted benzene ring triggered by a strong oxidant, NCS, in both stoichiometric and catalytic manners, affording compounds **2a** and **2b**, respectively. Compounds **1a**, **1b** and **2b** have been fully characterized by NMR spectroscopic and X-ray diffraction analyses. Preliminary radical scavenger studies suggest that the tandem C–Cl activation and dearomatization might go through a di-Pt(III) intermediate and the succinimide radicals can act as the chain carrier in the catalytic transformation of **1b** to **2b**. The possibility of applying the concept in this intramolecular reductive dearomatization onto an intermolecular system is being investigated in our group.

Experimental

General considerations

All preparations and manipulations were performed in air and all reagents were purchased from commercial sources and used without further purification. The L^{Et} and L^{F} ligands[6] and $[PtPh_2(SMe_2)]_n$ (n = 2 or 3)[7] were synthesized according to

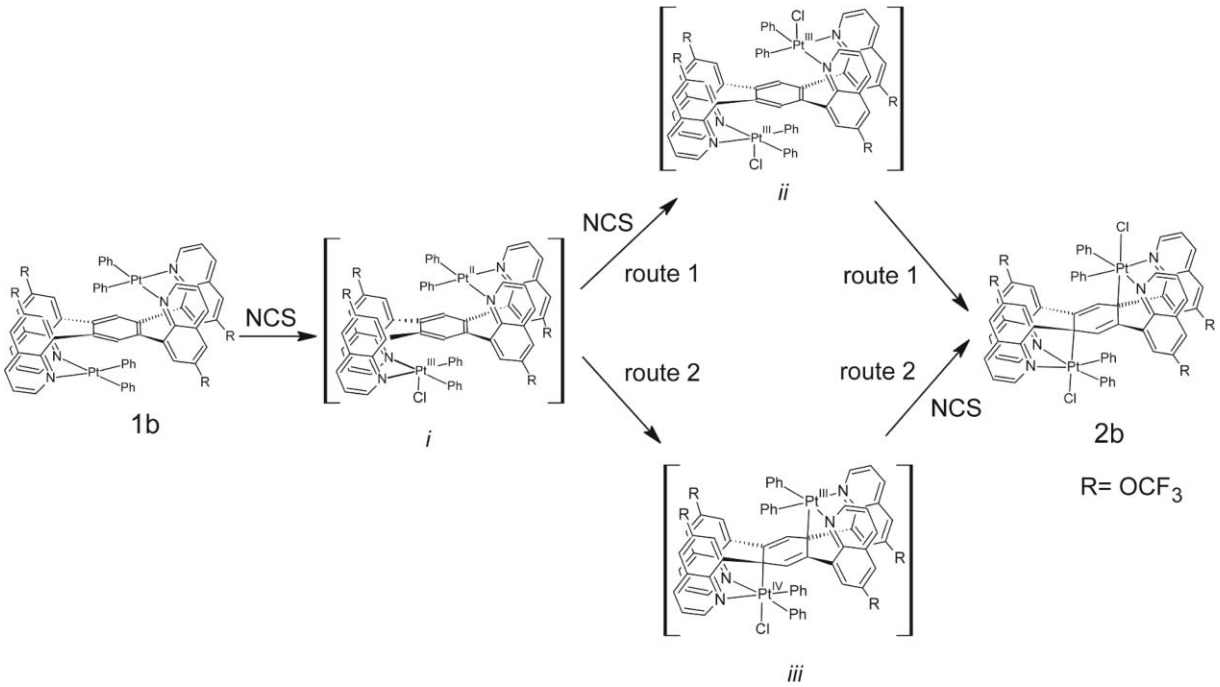

Scheme 4 Proposed mechanisms of the formation of **2b**.

literature procedures. ^{1}H and ^{19}F NMR spectra were recorded on a Varian 400 or a Bruker Avance 400 spectrometer. Chemical shifts were referenced relative to the solvent's residual signals but are reported relative to Me_4Si. Elemental analyses were performed on a PE 2400 C/H/N/S analyzer in our Chemistry Department.

Syntheses of 1a and 1b

L^{Et} (35 mg, 0.05 mmol) or L^{F} (46 mg, 0.05 mmol) was dissolved in 5 mL THF along with $[PtPh_2(SMe_2)]_n$ ($n = 2$, 42 mg, 0.05 mmol). The solution was stirred for 0.5 h at room temperature and then the solvent was removed under reduced pressure to yield an orange powder. Recrystallization from dichloromethane–hexanes gave the product as orange-yellow crystals (66.4 mg, 95% for **1a**; 72.3 mg, 90% for **1b**). **1a**: ^{1}H NMR (CD_2Cl_2, 400 MHz, 25 °C): δ 8.94 (dd, $^{3}J = 5.2$ Hz, $^{4}J = 1.6$ Hz, 4H), 7.98 (dd, $^{3}J = 8.0$ Hz, $^{4}J = 1.6$ Hz, 4H), 7.60 (s, 2H), 7.43 (d, $^{4}J = 2.0$ Hz, 4H), 7.32 (d, $^{4}J = 1.6$ Hz, 4H), 7.04 (dd, $^{3}J = 8.4$ Hz, $^{3}J = 4.8$ Hz, 4H), 6.78 (dd, $^{3}J = 8.0$ Hz, $^{4}J = 1.2$ Hz, 8H), 6.61–6.57 (m, 4H), 6.50–6.47 (m, 8H), 2.54–2.47 (m, 8H), 0.90 (t, $^{3}J = 7.6$ Hz, 12H). Anal. Calcd for $C_{74}H_{62}N_4Pt_2{\cdot}1/3CH_2Cl_2$: C 62.62, H 4.43, N 3.93. Found: C 62.86, H 4.62, N 3.91.

1b

^{1}H NMR (CD_2Cl_2, 400 MHz, 25 °C): δ 9.14 (d, $^{3}J = 4.2$ Hz, 4H), 8.18 (d, $^{3}J = 8.4$ Hz, 4H), 7.60 (s, 2H), 7.50 (d, $^{4}J = 2.0$ Hz, 4H), 7.43 (d, $^{4}J = 2.0$ Hz, 4H), 7.25 (dd, $^{3}J = 8.4$ Hz, $^{3}J = 4.2$ Hz, 4H), 6.75–6.70 (m, 10H), 6.63–6.59 (m, 10H). ^{19}F (CD_2Cl_2, 376 MHz, 25 °C): δ –58.46. Anal. Calcd for $C_{70}H_{42}N_4O_4F_{12}Pt_2{\cdot}1/2CH_2Cl_2$: C 50.90, H 2.61, N 3.37. Found: C 50.61, H 2.80, N 3.29.

Syntheses of 2a and 2b

1a (14 mg, 0.01 mmol) or **1b** (16 mg, 0.01 mmol) was dissolved in 2 mL of dichloromethane and *N*-chlorosuccinimide (2.6 mg, 0.02 mmol) was added into the solution. The reaction changed colour from orange to deep red immediately. After 30 minutes, an X-ray quality yellow crystalline product was formed, washed with dichloromethane, and dried in vacuum (8 mg, 55% for **2a**; 10 mg, 60% for **2b**).

Alternative route: compound **1b** (16 mg, 0.01 mmol) was suspended in 0.5 mL of $CDCl_3$ and *N*-chlorosuccinimide (0.26 mg, 0.002 mmol) was added into the suspension. The suspension turned into a clear solution within minutes. ^{1}H NMR indicated quantitative formation of **2b**.

2a

Anal. Calcd for $C_{74}H_{62}N_4Pt_2Cl_2{\cdot}1/3CH_2Cl_2$: C 59.65, H 4.22, N 4.11. Found: C 59.84, H 4.73, N 4.11.

2b

^{1}H NMR (CD_2Cl_2, 400 MHz, 25 °C): δ 9.82 (dd, $^{3}J = 4.8$ Hz, $^{4}J = 1.6$ Hz, 2H), 9.30 (dd, $^{3}J = 5.2$ Hz, $^{4}J = 1.6$ Hz, 2H), 8.43 (dd, $^{3}J = 8.4$ Hz, $^{4}J = 1.2$ Hz, 2H), 7.97 (dd, $^{3}J = 8.4$ Hz, $^{4}J = 1.6$ Hz, 2H), 7.86 (dd, $^{3}J = 8.4$ Hz, $^{3}J = 4.8$ Hz, 2H), 7.42 (s, 2H), 7.32 (dd, $^{3}J = 6.0$ Hz, $^{4}J = 3.6$ Hz, 2H), 7.25 (s, 2H), 7.05 (dd, $^{3}J = 8.0$ Hz, $^{3}J = 4.8$ Hz, 2H), 6.92–6.87 (m, 12H), 6.83 (d, $^{4}J = 2.4$ Hz, 2H), 6.76 (s, satellite, $^{3}J_{Pt-H} = 32.4$ Hz, $^{4}J_{Pt-H} = 16.4$ Hz, 2H), 6.42–6.38 (m, 4H), 5.98–5.95 (m, 4H). ^{19}F (CD_2Cl_2, 376 MHz, 25 °C): δ –57.95, –58.87. Anal. Calcd for $C_{70}H_{42}N_4O_4F_{12}Pt_2Cl_2{\cdot}CH_2Cl_2$: C 47.99, H 2.50, N 3.15. Found: C 48.24, H 2.64, N 3.24.

X-Ray diffraction analyses

X-Ray quality crystals of **1a** and **1b** were obtained by top-layering the CH_2Cl_2 solution with hexanes; those of **2a** and **2b** were obtained as described above. The crystals were attached to the tip of a MiTeGen MicroMount using Paratone oil and the single-crystal X-ray diffraction data were collected on a Bruker Kappa Apex II diffractometer with graphite-monochromated Mo Kα radiation ($\lambda = 0.71073$ Å), operating at 50 kV and 30 mA. All data were collected at 150 K controlled by an Oxford Cryostream 700 series low temperature system. Raw data were processed and multi-scan absorption corrections were applied using the Bruker Apex 2 software package.[12] All structures were solved by the direct methods and refined using SHELXTL V6.10.[13] Compounds **1a**, **2a**, and **2b** crystallized in the monoclinic space group $P2_1/n$ with 1, 0.5, and 0.5 molecule per asymmetric unit, respectively, while **1b** crystallized in the monoclinic space group $C2/c$ with 0.5 molecule per asymmetric unit. THF molecules were found in the lattice of **1a** (1 molecule of THF per molecule of **1a**); CH_2Cl_2 molecules were found in the lattice of **2a** (2 molecules of CH_2Cl_2 per molecule of **2a**); disordered CH_2Cl_2 molecules were found in the lattice of **2b** (2 molecules of CH_2Cl_2 per molecule of **2b**). Two of the quinolinyl moieties and the attached ethyl groups in **1a**, one of the CF_3 groups in **1b**, the ethyl groups in **2a**, and one phenyl ligand and one quinolinyl group and the attached OCF_3 group in **2b** are disordered. All these disordered portions were modelled successfully. During the modelling process for the disordered ethyl group in **2a**, 5 least-squares restraints were used. The residual electron density from disordered, unidentified solvent molecules in the lattice of **1b** was removed with the SQUEEZE function of PLATON program[14] and their contributions were not included in the formula. Elemental analysis results suggest that CH_2Cl_2

Table 1 Crystallographic data

	1a·C_4H_8O	**1b**	**2a**·$2CH_2Cl_2$	**2b**·$2CH_2Cl_2$
Formula	$C_{78}H_{70}N_4OPt_2$	$C_{70}H_{42}F_{12}N_4O_4Pt_2$	$C_{76}H_{66}Cl_6N_4Pt_2$	$C_{72}H_{46}Cl_6F_{12}N_4O_4Pt_2$
FW	1469.56	1261.26	1638.21	1862.01
T/K	150(2)	150(2)	150(2)	150(2)
Space group	$P2_1/n$	$C2/c$	$P2_1/n$	$P2_1/n$
a/Å	13.8443(8)	32.542(2)	10.213(1)	10.0461(2)
b/Å	20.558(1)	11.957(1)	21.299(2)	21.5220(4)
c/Å	21.305(1)	21.378(2)	15.109(1)	15.2720(4)
α/°	90	90	90	90
β/°	97.934(3)	127.996(4)	98.108(4)	96.650(1)
γ/°	90	90	90	90
V/Å^3	6005.5(6)	6555.3(9)	3253.5(5)	3279.8(1)
Z	4	4	2	2
ρ_{calcd}/g cm^{-3}	1.625	1.643	1.672	1.885
μ/mm^{-1}	4.706	4.348	4.590	4.595
No. reflns collcd	49 767	26 365	28 097	28 705
No. indept reflns	12981	7108	7404	7506
GOF on F^2	1.011	0.997	1.009	1.011
R [$I > 2\sigma(I)$]	$R_1 = 0.0568^a$	$R_1 = 0.0378^a$	$R_1 = 0.0472^a$	$R_1 = 0.0368^a$
	$wR_2 = 0.1104^b$	$wR_2 = 0.0896^b$	$wR_2 = 0.0763^b$	$wR_2 = 0.0736^b$
R (all data)	$R_1 = 0.1367$	$R_1 = 0.0635$	$R_1 = 0.1064$	$R_1 = 0.0619$
	$wR_2 = 0.1392$	$wR_2 = 0.0959$	$wR_2 = 0.0932$	$wR_2 = 0.0817$

^{a} $R_1 = \sum(F_o - F_c)/\sum F_o$. ^{b} $wR_2 = [\sum[w(F_o^2 - F_c^2)^2]/\sum w(F_o^2)^2]^{1/2}$.

Table 2 Selected bond lengths (Å) and angles (°)

1a		**1b**		**2a**		**2b**	
Pt(1)–C(45)	2.00(1)	Pt(1)–C(24)	1.998(6)	Pt(1)–C(29)	2.047(7)	Pt(1)–C(21)	2.038(5)
Pt(1)–C(51)	2.03(1)	Pt(1)–C(30)	2.034(5)	Pt(1)–C(23)	2.052(7)	Pt(1)–C(27)	2.057(5)
Pt(1)–N(1)	2.174(8)	Pt(1)–N(1)	2.150(4)	Pt(1)–N(1)	2.159(5)	Pt(1)–N(1)	2.161(4)
Pt(1)–N(2)	2.149(8)	Pt(1)–N(2)	2.172(4)	Pt(1)–C(35)	2.139(8)	Pt(1)–C(33)	2.138(4)
C(45)–Pt(1)–C(51)	91.6(4)	C(24)–Pt(1)–C(30)	91.3(2)	Pt(1)–N(2)	2.147(5)	Pt(1)–N(2)	2.21(1)
C(45)–Pt(1)–N(2)	88.7(4)	C(24)–Pt(1)–N(1)	88.9(2)	Pt(1)–Cl(1)	2.462(2)	Pt(1)–Cl(1)	2.443(1)
C(51)–Pt(1)–N(2)	177.5(4)	C(30)–Pt(1)–N(1)	175.2(2)	C(35)–C(37)#1	1.49(1)	C(33)–C(35)#2	1.486(7)
C(45)–Pt(1)–N(1)	166.1(4)	C(24)–Pt(1)–N(2)	166.8(2)	C(35)–C(36)	1.494(9)	C(33)–C(34)	1.480(7)
C(51)–Pt(1)–N(1)	92.9(4)	C(30)–Pt(1)–N(2)	95.5(2)	C(36)–C(37)	1.342(9)	C(34)–C(35)	1.352(7)
N(1)–Pt(1)–N(2)	86.2(3)	N(1)–Pt(1)–N(2)	83.4(2)	C(37)#1–C(35)–C(36)	113.4(6)	C(35)#2–C(33)–C(18)	111.3(6)
				C(37)#1–C(35)–C(8)	108.6(6)	C(34)–C(33)–C(18)	108.7(5)
				C(36)–C(35)–C(8)	111.6(6)	C(34)–C(33)–C(35)#2	111.3(6)
				C(37)#1–C(35)–Pt(1)	110.7(5)	C(35)#2–C(33)–Pt(1)	110.3(3)
				C(36)–C(35)–Pt(1)	110.1(5)	C(34)–C(33)–Pt(1)	110.3(3)
				C(8)–C(35)–Pt(1)	101.9(4)	C(18)–C(33)–Pt(1)	102.1(4)

#1: $1 - x + 3, -y + 1, -z + 1$; #2: $-x, -y, -z + 1$.

co-crystallized with **1b**. All non-hydrogen atoms except for the atoms involved in the disordered portions were refined anisotropically. The positions of the hydrogen atoms were calculated using the riding model. Selected crystallographic data are presented in Table 1, while selected bond lengths and angles are listed in Table 2.

Acknowledgements

This research is supported by grants to D. S. from the Canadian Foundation for Innovation, Natural Sciences and Engineering Research Council of Canada, Ontario Ministry of Research and Innovation, the University of Toronto, Connaught Foundation. R. T. is grateful for a postgraduate scholarship from the OGS program of Ontario.

Notes and references

1 J. D. Hepworth, *Aromatic chemistry*, Royal Society of Chemistry, Cambridge, 2002.
2 (*a*) A. J. Birch and H. Smith, *Q. Rev. Chem. Soc.*, 1958, **12**, 17; (*b*) T. J. Donohoe and D. House, *J. Org. Chem.*, 2002, **67**, 5015; (*c*) M. C. Cassani, Y. K. Gun'ko, P. B. Hitchcock and M. F. Lappert, *Chem. Commun.*, 1996, 1987.
3 (*a*) G. C. Dismukes, *Chem. Rev.*, 1996, **96**, 2909; (*b*) C. Belle and J. Pierre, *Eur. J. Inorg. Chem.*, 2003, 4137; (*c*) P. C. Dos Santos, D. R. Dean, Y. Hu and M. W. Ribbe, *Chem. Rev.*, 2004, **104**, 1159.
4 D. Song, K. Sliwowski, J. Pang and S. Wang, *Organometallics*, 2002, **21**, 4978.
5 D. Song and S. Wang, *Comments Inorg. Chem.*, 2004, **25**, 1.
6 R. Tan, P. Jia, Y. Rao, W. Jia, A. Hadzovic, Q. Yu, X. Li and D. Song, *Organometallics*, 2008, **27**, 6614.
7 D. Song and S. Wang, *J. Organomet. Chem.*, 2002, **648**, 302.
8 S. R. Whitfield and M. S. Sanford, *J. Am. Chem. Soc.*, 2007, **129**, 15142.
9 S. R. Whitfield and M. S. Sanford, *Organometallics*, 2008, **27**, 1683.
10 D. D. Tanner, D. W. Reed, S. L. Tan, C. P. Meintzer, C. Walling and A. Sopchik, *J. Am. Chem. Soc.*, 1985, **107**, 6576.
11 L. R. Mahoney, *J. Am. Chem. Soc.*, 1966, **88**, 3035.
12 Apex 2 Software Package; Bruker AXS Inc. 2008.
13 G. M. Sheldrick, Acta, Crystallogr., Sect. A: Found, *Crystallogr*, 2008, **64**, 112.
14 A. L. Spek, *J. Appl. Crystallogr.*, 2003, **36**, 7.